Jour. Fac. Sci., Hokkaido Univ., Ser. VII (Geophysics), Vol. 9, No. 5, 463-479, 1995.

Doppler Radar Observations of Orographic Effects of Isolated Echoes during the Baiu Season at Nagasaki Prefecture, on July 14 and 15, 1988

Nobuhiro Takahashi*, Hiroshi Uyeda, Katsuhiro Kikuchi and Koyuru Iwanami**

Department of Geophysics, Faculty of Science, Hokkaido Univerity, Sapporo 060, Japan

(Received November 17, 1994)

Abstract

The behavior of isolated convective echoes and orographic effects on the echo development were analyzed for the cases of July 14 and 15 in 1988 observed by using an X-band Doppler radar, at Saikaicho, Nagasaki Prefecture.

From the analysis, each isolated echo which consisted of several echo cells had a life time more than 120 minutes and developed well enough to provide heavy rainfall under the environment of late period of the Baiu season. Volume scan data also showed the potential of isolated echoes for strong rainfall.

An orographic effect was examined by comparing with echoes of different passes during their development : one echo passed over mountain area and the other passed over relatively flat area. The analysis revealed that rapid development appeared at the mountain area and the strong rainfall occurred at the mountain area. This result was explained to be caused by the fact that the echo developed so quickly that the echo produced much rain drops there, and the echo reached downdraft stage at the mountain area. Detailed mechanisms of the orographic effect, barrier effect and changing of wind direction, were revealed by dual Doppler radar analysis.

1. Introduction

In the late period of the Baiu season, many heavy rainfall events had occurred along the Baiu front in the western part of Japan. These heavy

* Present affiliation : Communications Research Laboratory, Kashima, Ibaraki Pref., 314.

** Present affiliation : Nagaoka Institute of Snow and Ice Studies, National Research Institute for Earth Science and Disaster Prevention, Nagaoka, Niigata Pref., 187-16

rainfalls regularly concentrated in a limited area such as meso-β or meso-γ scales. These heavy rainfalls were caused by well developed and organized convective clouds. For the concentration mechanisms of heavy rainfalls, the major mechanisms are considered to be the organization process of the Baiu frontal rainband and the orographic and/or topographic effects. The Baiu frontal heavy rainfalls are often induced by the mesoscale convective system (or cloud cluster from the satellite observation) (Akiyama, 1984a, b ; Ogura et al., 1985 ; Harimaya et al., 1989 ; Kato and Harimaya, 1989 ; Takeda and Iwasaki, 1989) and the effect of complex configuration of Japan on the cloud development cannot be ignored (Ogura et al., 1985 ; Watanabe and Ogura, 1987). Ogura et al. (1985), who analyzed the historical heavy rainfall event on Nagasaki in 1982 (called Nagasaki event) using conventional radar and GMS data, suggested that the blocking effect of mountains played an important role for the long lasting heavy rainfall around Nagasaki City in 1982 ; Nagasaki locates west of the mountains. In their study, meso-β scale organization process was a merging between blocked cloud cluster and newly generated cloud at the western edge of the cloud cluster (in their case, Nagasaki located just east of the merging point). On the other hand, Takahashi (1994) emphasized the importance of the gust fronts (outflow from convective cloud) from a Doppler radar observations of convective cloud in July 1988 at Nagasaki Prefecture ; gust front contributed for enhancement of the Baiu frontal convergence zone and its propagation direction (north to south, while the environmental wind was westerly) caused the effective merging ; echo significantly developed after merging. In his case study, Doppler radar observations made it clear to understand the organization process. These studies suggested the importance of the development of each convective cloud or convective cell. It was emphasized, therefore that the estimation of the potentiality of convective cell for rainfall amount was very important.

In this study, a development process of isolated convective echo cells is analyzed in order to clarify the potential influence of the Baiu frontal environment on convective cloud development. Isolated echoes to be analyzed are cases of July 14 and 15, 1988. For this analysis, Hokkaido University X-band Doppler radar data was mainly utilized ; Doppler radar provides not only reflectivity of echoes but also wind field inside the echo. The advantage for selecting isolated echo is that it has relatively simple structure.

An orographic effect was also examined by comparing with two isolated echoes under almost same environment on their life cycle, circulation mechanism, and potential of rain production : one passed over mountain area, and the

other passed over plain. Ogura et al. (1985) and Watanabe and Ogura (1987) focused on the meso-α or meso-β scale orographic effects, while horizontal scale of the orographic effect in this study focused on meso-γ scale effect because the scale of the target echo was very small ($\approx$20 km). This study provides more detailed process of the orographic effect. The orographic effect on an isolated echo was also examined by dual Doppler radar analysis by using Hokkaido University (HU) Doppler radar and Meteorological Research Institute (MRI) Doppler radar.

2. Observation and environmental conditions

Doppler radar observations were performed from July 7 to 20, 1988, by using HU X-band Doppler radar at Saikaicho, Nagasaki Prefecture, as a part of cooperative observation of heavy rainfall event at the late period of the Baiu season (Asai, 1990). During the observation, 3 or 6 hourly sounding data, including special sounding points of Fukue and Kumamoto, was available. Figure 1 shows the location of HU Doppler radar with 60 km observation range (solid line circle), and MRI Doppler radar with 60 km observation range (dashed line circle). This figure also shows the location of three sounding points of Fukuoka, Kumamoto, and Fukue by solid squares. In this study, only sounding data

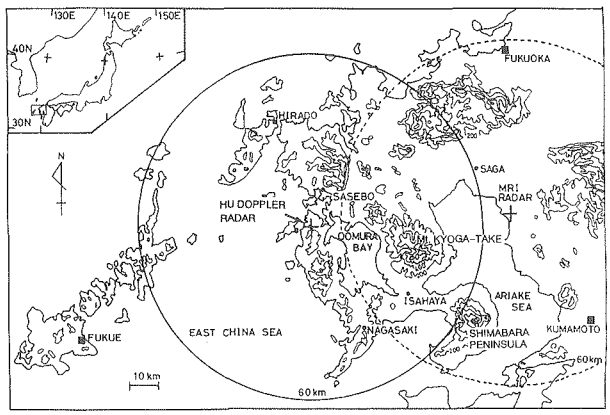

Fig. 1. Map of the observation area with sounding stations (Fukuoka, Fukue, and Kumamoto) expressed as solid squares and topography shown with 200 m contour intervals. The location of the Hokkaido University Doppler radar and its 60 km range is depicted as a cross encircled by a solid line. The location of the MRI radar and its 60 km range is depicted as a cross encircled dashed line. Weather station locations are shown as solid circles.

of Fukue was used as the environmental value (the reason will be mentioned later). From the viewpoint of topography, an observation area is very complicated: mountain area located south and north of the radar site, and about 1,000 m height mountain (Mt. Kyoga-take) located about 40 km east of the radar site. In the case of July 15, the echo passed over the mountain area as shown in Fig. 2 by solid triangles connected by solid line. On the other hand, the echo of July

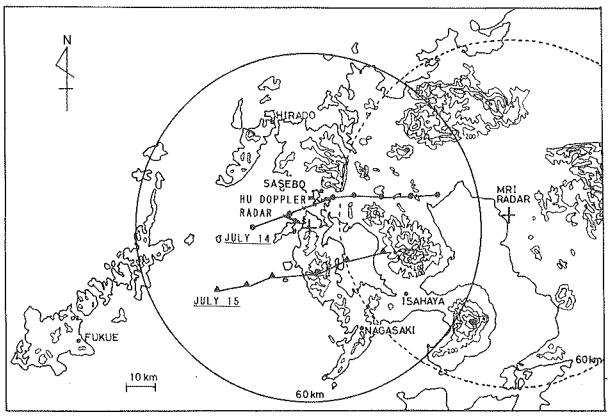

Fig. 2. The paths of the isolated echoes on July 14 (●) and July 15 (▲), 1988. Symbols express the location of the echoes at about 15 minute intervals starting from 1015JST on July 15, and at about 15 minute intervals starting from 1315JST on July 14. The echoes were traced using CAPPI (2 km) reflectivity data.

Table 1. Specification of the Hokkaido University Doppler radar.

Kokkaido Univ. Meteor. Lab. Doppler Radar		
Parameter	Doppler	Conventional
Wave length (cm)	3.2	3.2
Maximum range (km)	63.5	63.5
Nyquist velocity (m/s)	±12.0	—
Pulse duration (μs)	0.4	0.8
Pulse repetition frequency (Hz)	1,500	750
Azimuthal resolution (deg.)	0.7	1.0
Beam width (deg.)	2.0	2.0
Number of samples	254	254
Gate spacing (m)	62.5	62.5
Sample spacing (m)	250	250
Antenna rotation (rpm)	1	4
Antenna diameter (m)	1.2	1.2

14, passed over plain region by solid circles connected by solid line.

The specification of the HU Doppler radar was presented in Table 1. During the observation, two kinds of mode were utilized: one is conventional mode in order to survey the three dimensional structure of the echo by volume scan, the other is Doppler mode in order to survey the low level wind field (PPI scan) and vertical circulation within the echo (RHI) scan. Both modes have range resolution of 250 m. The observation was performed 15 minute intervals: volume scan with 15 elevation angles and a few low elevation angles of Doppler mode PPI scans and RHI scans.

Data analysis was mainly performed by using single Doppler radar, a dual Doppler analysis was realized only for the echo of July 15 at the mountain region, because of regional restriction of dual Doppler analysis.

Figure 3 expresses the synoptic situations of July 14 and 15 by surface weather maps. The Baiu front located north of Kyushu, and a subtropical high dominated the Kyushu area. This configuration is typical in the late period of the Baiu season; the Baiu front was characterized as weak discontinuity of wind and temperature, and relatively large gradient of water vapor, and water vapor is supplied from the southern sea area of the Baiu front at the western edge of tropical high pressure system. Figure 4 presents the vertical profiles of potential temperature (θ), equivalent potential temperature (θ_e), and saturated equivalent potential temperature (θ_e^*) at 15JST on July 14 and at 09JST on July

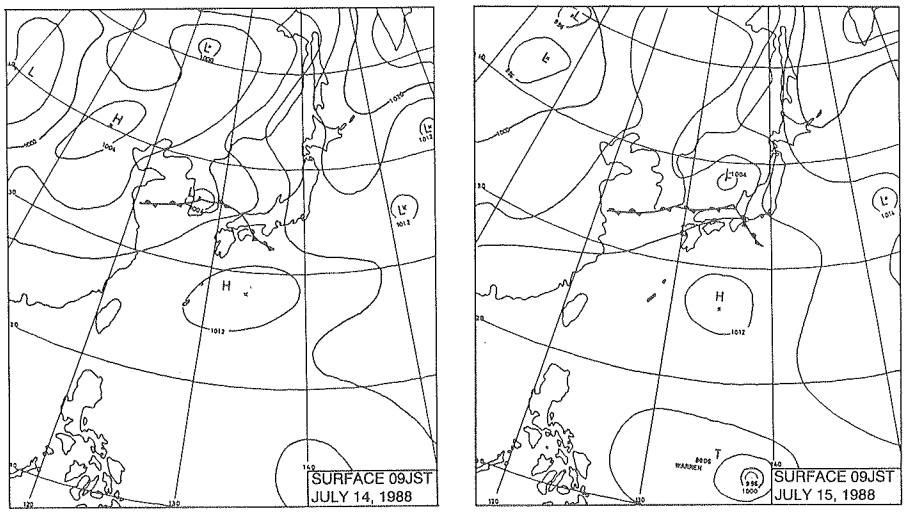

Fig. 3. Surface weather maps for 09JST on July 14 and 15, 1988.

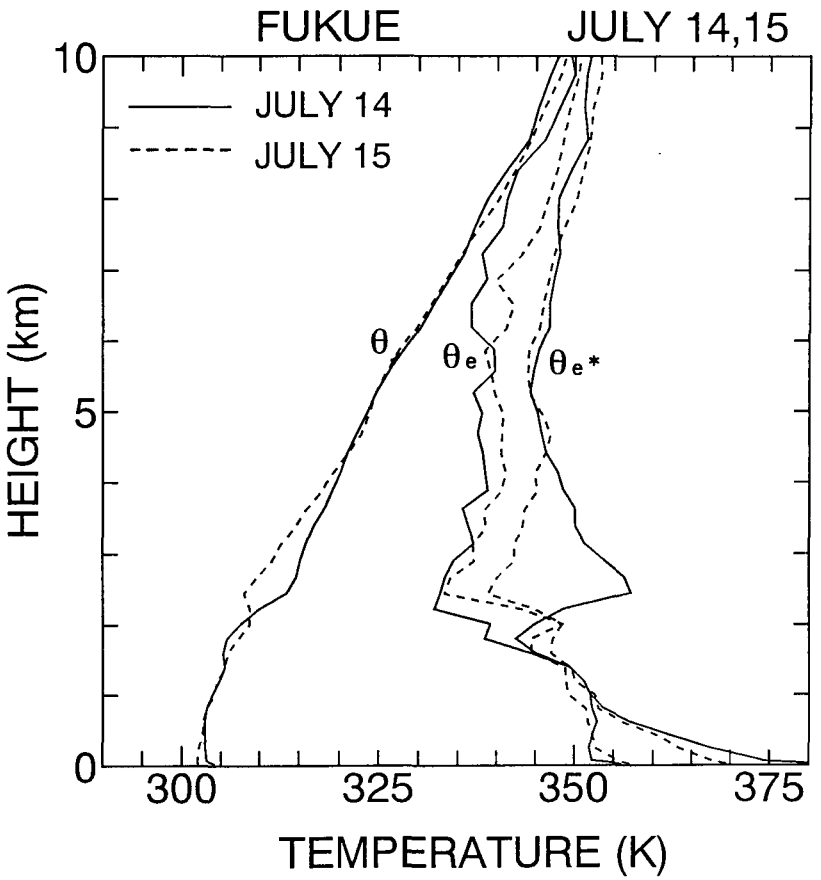

Fig. 4. Vertical profiles of potential temperature (θ), equivalent potential temperature (θ_e) and saturated equivalent potential temperature (θ_e^*) at Fukue at 15 JST on July 14 and 09JST on July 15, 1988.

15 (the closest sounding time for both cases) at Fukue. Since echoes generated on the East China Sea, the closest sounding point was Fukue, for these cases. A convectively unstable layer existed below 2.3 km in height on both days; a relatively dry layer existed at 2.5 km on July 14. Calculated CAPE (Convective Available Potential Energy) values for July 14 and July 15 are 1,370 J/kg and 2,250 J/kg, respectively. These values suggest that the echoes on July 15 had greater convective energy than those of July 14.

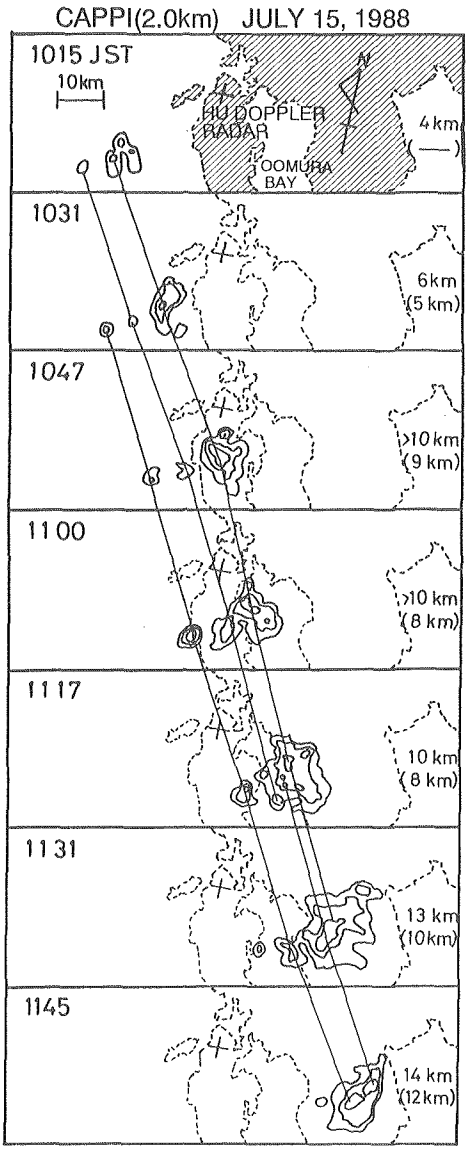

Fig. 5. The transition of the isolated echoes on July 15, 1988, as a series of CAPPI at 2 km in height. Numbers in each frame indicate the echo top height at a threshold reflectivity of 18 dBZ (parenthesis: for 27 dBZ). Contour interval is 6 dBZ from 18 dBZ.

3. Echo development process

The developments of these two echoes are traced continuously. Figure 2 displays the courses of the echoes of both July 14 and 15 cases. The July 15 echo passed over two mountain areas while the July 14 echo passed over plain. Figure 5 presents the transition of the July 15 isolated echo as a series of CAPPI at 2 km in height. The echo initially appeared over the sea which was consisted of several echo cells and moved to the east-northeast at a speed of 10 ms^{-1}, with the echo area increasing monotonous. The echo landed between 1031JST and 1047JST, moving over Oomura Bay at 1117JST; finally landed again and reached mountain area (Mt. Kyoga-take) at around 1140JST. Figure 5 also presents the echo top height of the threshold reflectivities of 18dBZ and 27dBZ (in parenthesis) on the right portion of each panel. Rapid increases in echo top height appeared when the echo landed on (1031 and 1117JST) mountains. The transition of the July 14 echo is presented in Fig. 6 in the same manner as Fig. 5. Figure 6 shows that this echo landed at 1407JST, but in this case rapid development did not occur.

The difference in the develop-

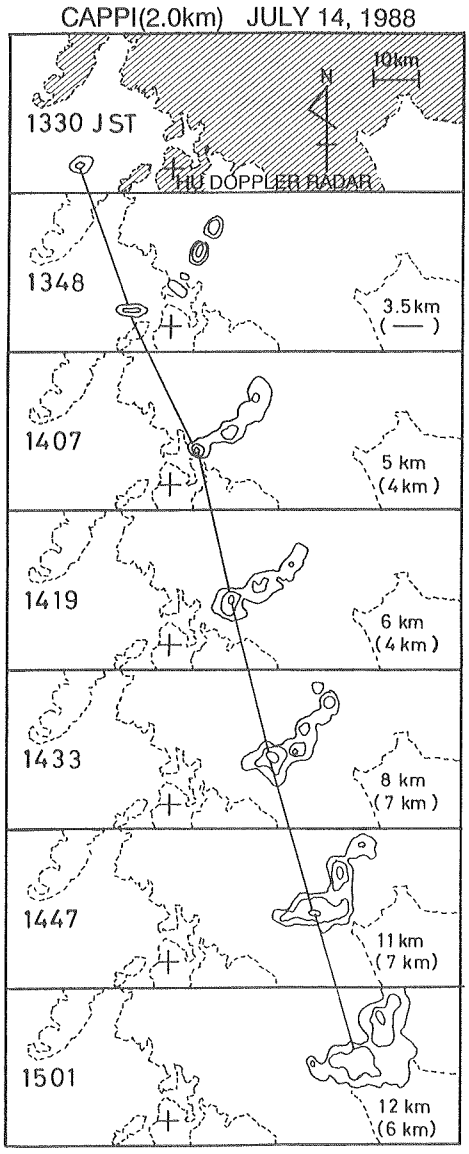

Fig. 6. The transition of the isolated echo on July 14, 1988 as a series of CAPPI at 2 km in height. Numbers in each frame indicate the echo top height at a threshold reflectivity of 18 dBZ (parenthesis: for 27 dBZ). Contour interval is 6 dBZ from 18 dBZ.

ment processes of the July 14 and July 15 cases is summarized with their echo top height in Fig. 7. Landing times of the echoes are indicated by arrows. The July 15 echo had a longer life cycle than that of July 14. In the July 15 case, a rapid echo development coincided with landing. Between the first and the second rapid development stages, the 27dBZ echo top height slightly decreased. On the other hand, the 18dBZ echo top height of the July 14 echo developed monotonously. Duration of echo top height less than 5 km ($\approx$0°C level) varies from 20 minutes to 40 minutes because of the degree of landing effect. This value may express the duration of warm rain stage. If so, these results coincide with an isolated echo in a tropical island (Takahashi and Uyeda, 1995). In this case study, however, the transition process between warm rain and cold rain was not clarified from this analysis.

The life cycle of the July 15 echo was determined using the low altitude echo area and the divergence field derived from low elevation angle PPI data. Figure 8 represents the transition of the echo and divergence/convergence (radial divergence/convergence; calculated by the radial gradient of Doppler velocity) areas. This

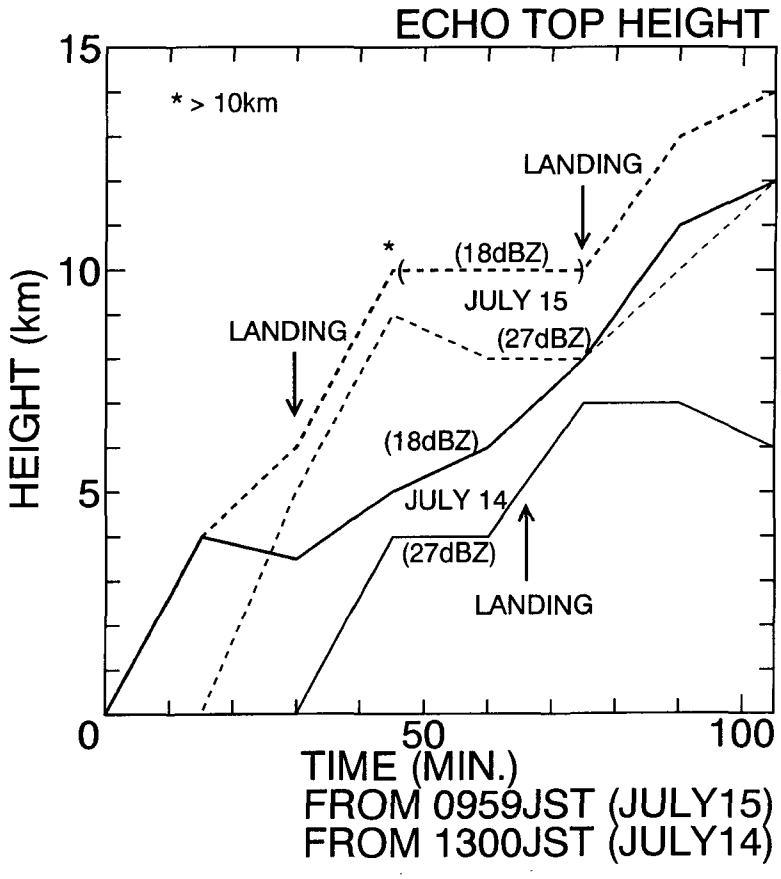

Fig. 7. Time versus echo top height of the isolated echoes. The bold solid (dashed) line expresses the case of July 14 (15) with a threshold reflectivity of 18 dBZ. The thin solid (dashed) line expresses the case of July 14 (15) with a threshold reflectivity of 27 dBZ. Landing times are indiated by arrows.

figure shows that the divergence area occupied slightly larger than convergence area through the life. It comes from the difference between divergence and convergence intensity; convergence was more intense than divergence in this case. When a rapid increase in echo area took place at the landings (70 and 110 minutes), divergence significantly dominated the low altitude wind field after the first landing. It was caused by a downdraft which was forced by heavy rain water loading (stronger reflectivity coincides with larger amounts of rainwater in the echo).

Vertical cross sections of reflectivity with 2-dimensional circulation before

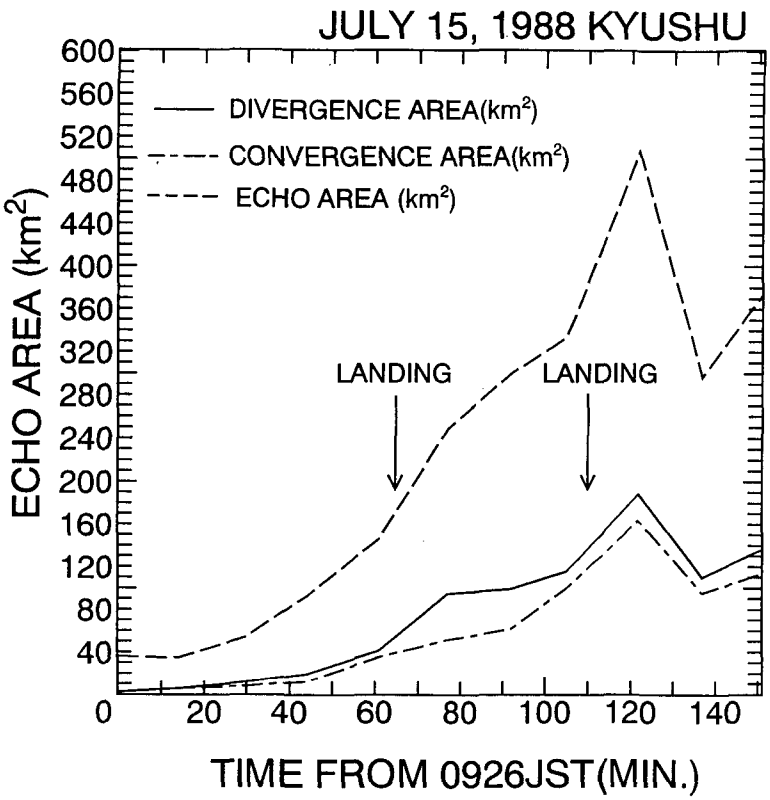

Fig. 8. The transition of echo area and divergence (convergence) area for the case of July 15, 1988.

and after landing are presented in Figs. 9 (July 15) and 10 (July 14). The vertical wind component was calculated by integrating the radial divergence in the RHI scan frame. In Fig. 9, the echo was dominated by updraft just before landing, while downdraft dominated after landing. This drastic change in cloud circulation was caused by an orographic effect; that is, a mountain slope resulted in upward forcing triggering rapid echo development. In such moist environments as the Baiu frontal region, an echo grows rapidly even due to weak forcing (updraft). Updraft causes water condensation to release latent heat. This process enhances the strength of the updraft. Therefore, in this case, as a result of rapid development, much rain water was produced in the echo and was sustained by the strong updraft. After passing over the slope, the updraft no longer sustained the echo because of the high rain water content in the echo and

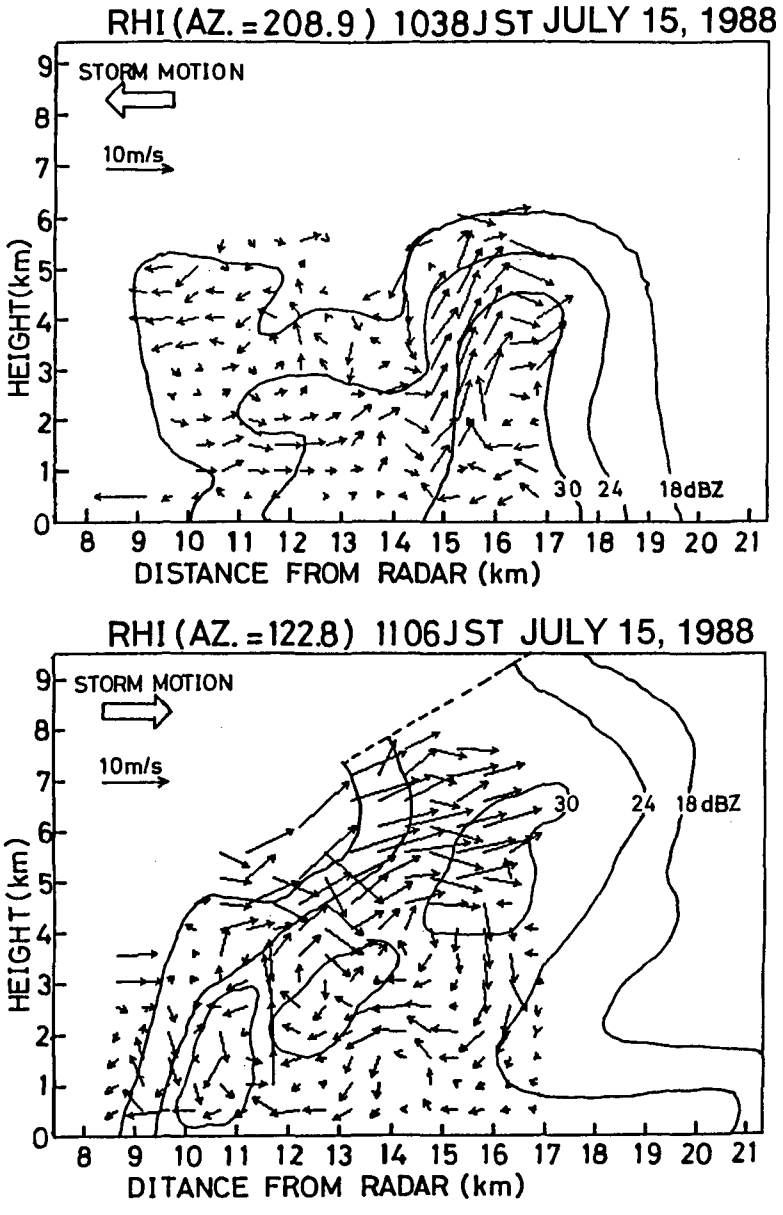

Fig. 9. Vertical cross sections (RHI scan) of echo. Upper frame: 1038JST (before landing). Lower frame: 1106JST (after landing) on July 15, 1988. Two dimensional wind fields derived from Doppler velocity are superimposed on the reflectivity frames.

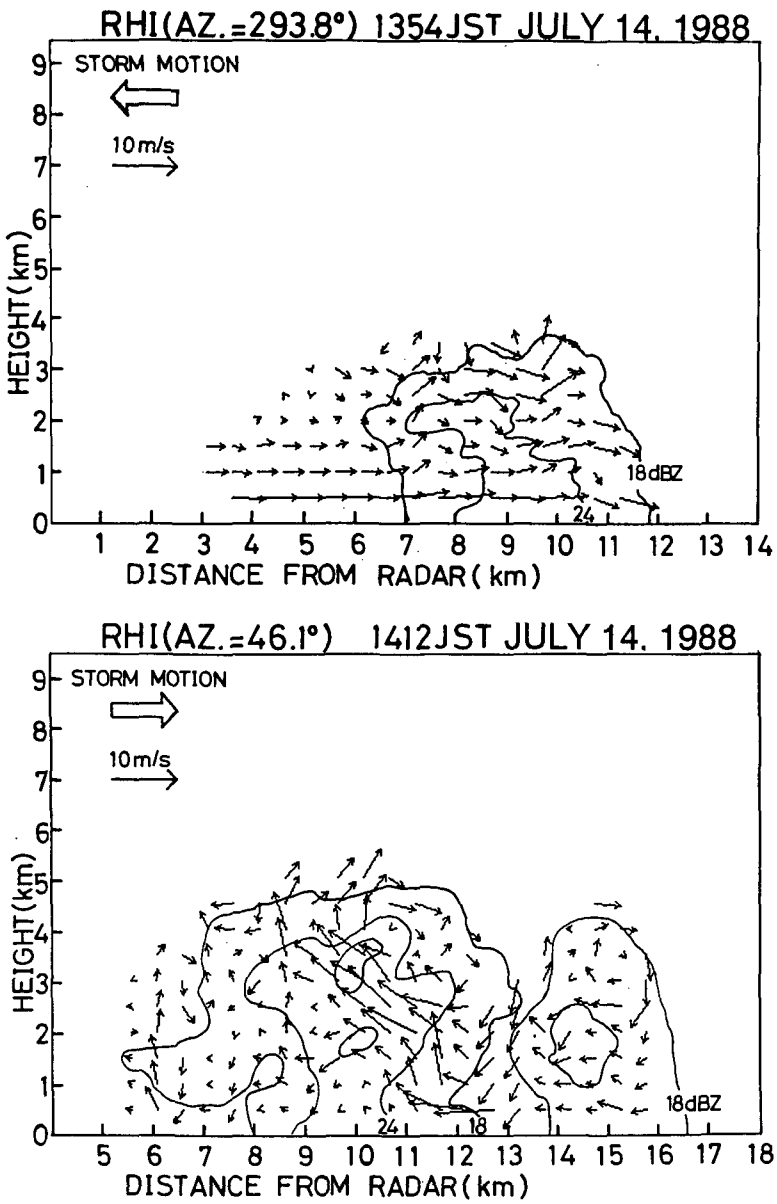

Fig. 10. Vertical cross sections (RHI scan) of echo. Upper frame: 1354JST (before landing). Lower frame: 1412JST (after landing) on July 14, 1988. Two dimensional wind fields derived from Doppler velocity are superimposed on the reflectivity frames.

the weakening of the updraft. Then, a strong downdraft was initiated. As mentioned in the discussion of Fig. 7, the echo developed again when it reached a mountain area. This result suggests that if the second mountain area did not lie under the echo path, the echo would have decayed just after passing over the first mountain area. However, the echo developed again rapidly at the second mountain area. In the July 14 case (Fig. 10), a circulation within the echo did not exhibit a drastic change during its life cycle. The circulation sustains the monotonous development of the echo. The results of this comparison indicate that mountains force rapid echo development, accelerating echo development and dissipation.

4. *Estimation of orographic effect on rainfall amount*

Using the volume scan data, three dimensional rain water amount was

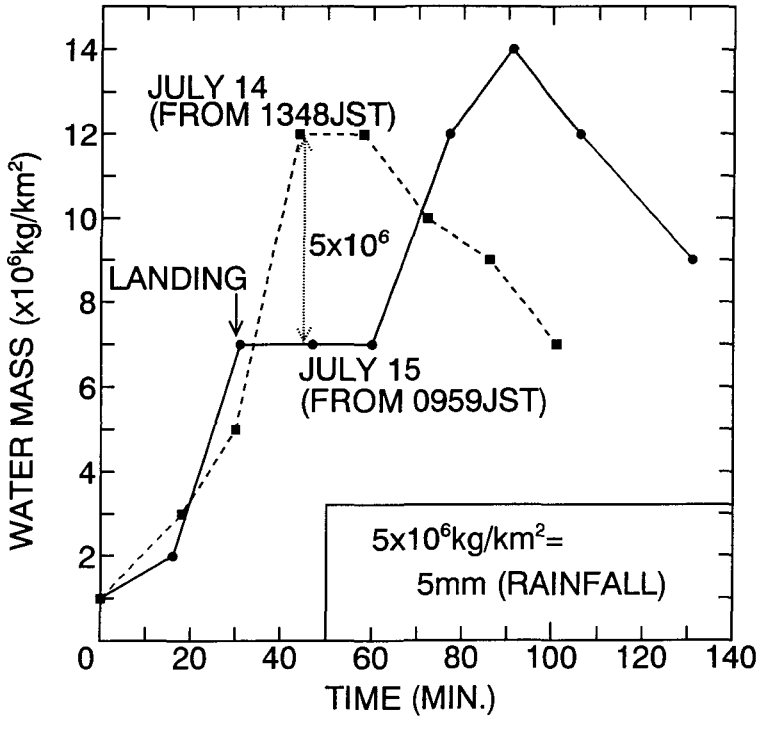

Fig. 11. Temporal variation in total rain water mass of the case on July 14 (dashed line) and July 15 (solid line), 1988.

estimated for both echoes. The formula for the estimation is $Z=3.8\times10^{2}\,M^{1.46}$ (Brown and Braham, 1963), where Z(mm^{6}·m^{-3}) is reflectivity factor and M(g·m^{-3}) is liquid (rain) water content. Figure 11 expresses rain water transition for both cases. Both echoes contained rain water more than 10×10^{6} kg/km^{2}; this value is equivalent to the 10 mm of rainfall amount. It is supposed that the changes in rainwater is almost connected to the changes in echo top height. In this case study, July 14 echo represents the normal echo (non-orographic effect) and July 15 echo is affected by orographic effect. The difference in rain water amount in Fig. 11 (5×10^{6} kg/km^{2}) from that produced from the development of an average echo (such as the July 14 echo) is due to the mountain effect; this difference was supplied to the mountain area (5 mm of rainfall). This is confirmed by AMeDAS surface observation (5 mm rainfall from 10JST to 11JST at Ooseto, which is located on the landing point of the July 15 echo).

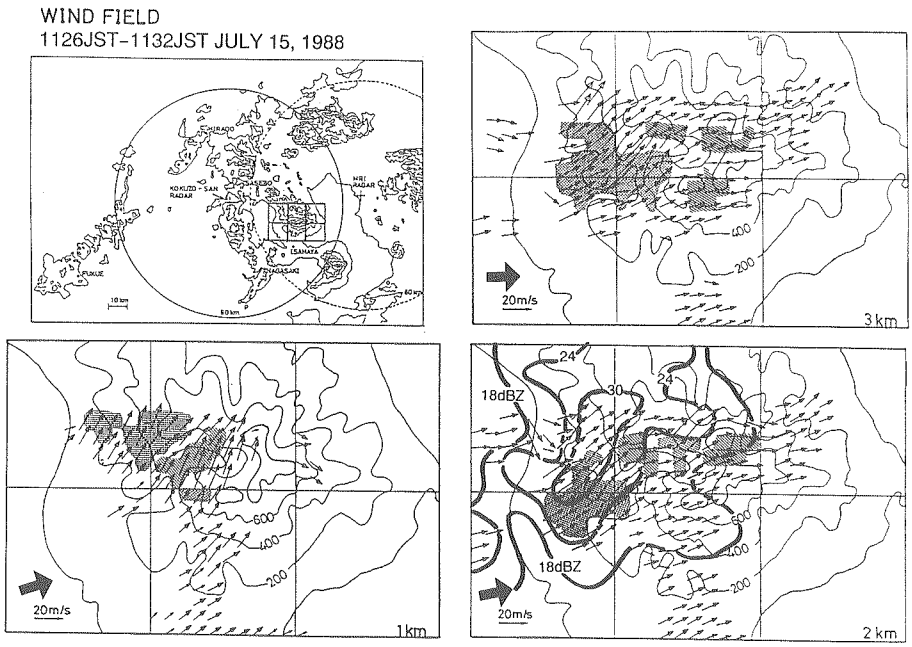

Fig. 12. Wind field at 1 km, 2 km, and 3 km in height around the mountain area (expressed as squares in the map) derived by dual Doppler analysis. Thin contours express the topographical countour with a 200 m interval. For the 2 km frame, bold contour expresses the reflectivity; contour interval is 6 dBZ from 18 dBZ. Hatched area represents divergence greater than 10^{-3} s^{-1} and stippled area represents convergence greater than 10^{-3} s^{-1}. Environmental wind directions are expressed by the bold arrow.

Differences in the effect of landing were caused by differences in the gradients of the slope on the landing places. As shown in Fig. 2, the July 15 echo passed over two mountain areas; one is about 400 m in height and the other is about 1,000 m in height. On the other hand, the July 14 echo passed over land less than 200 m in height throughout its life cycle.

Since the barrier effect of mountains is considered to be the main reason for rapid development of the echo, the wind field at the mountain area is examined using dual Doppler analysis for the July 15 case (Fig. 12). The wind field is calculated for 1 km, 2 km, and 3 km in height around Mt. Kyoga-take (see Fig. 1), which has a peak height of 1,000 m. At 1 km in height, the wind field was calculated only for the area west of the mountain. Since wind direction in this area was south-southwesterly though the sounding data indicates that the environmental wind direction was west-southwest at 1 km in height, it is assumed that the wind flowed around the mountain area. A convergence zone was located west of the mountain peak. At 2 km in height, a convergence region existed over the mountain. The divergence region coincided with the strong reflectivity region. The mountain effect on the wind field at 3 km in height was not clear. In any case, mountains affect echoes by acting as a barrier, forcing air streams to go around them and causing convergence above them.

The change in wind direction resulting from the barrier effect caused the change of echo propagation direction, and the convergence effect leads to the development of an echo above the mountain. This effect is very important when we consider "heavy rainfall in a limited area". Because the ability of one echo to bring rainfall is limited, the successive passage of echoes over the same area is very important. The mountain effect therefore contributes to this by leading echoes to specific places, such as the flank of a mountain at Isahaya City.

The results of this case study indicate that the mountains have two effects. One is rapid echo development (rapid production of rainwater) in mountain areas, the other is the barrier effect, which changes the course of an echo propagation such as Kikuchi et al. (1994). Both effects are assumed to partially contribute to heavy rainfall in a limited area.

5. Concluding remarks

In this study, a behavior of isolated clouds and orographic effect during the Baiu season were examined by using Doppler radars. During the late period of the Baiu season, isolated echoes often generated over the sea at the south of the

Baiu front in which the environmental conditions were warm and moist. The isolated echoes which were consisted of several echo cells had more than 120 minutes in life cycle and sometimes reached maximum echo top height of 15 km. These echoes had potentiality for the rainfall amount of more than 10 mm. And the existence of warm main process was suggested from the analysis; it will be clarified by cloud physical observations, such as multi-parameter radar or aircraft observations.

The orogaphic effect on the convective cloud was explained in this study comparing with two cases of the isolated echoes: one passed over a mountain area and the other passed over on the plain. The orographic effect appeared as rapid development of the echo at the mountain slope. It caused more rainfall at the mountain area than other areas, in other words, an echo development was urged at the mountain area; rain water amount in the echo constantly increased in the case in which the echo passed over non-mountain area, but the echo which passed over mountains brought rain water as precipitation to the ground which should be stored within the echo. The difference between the echo with ordinary development and the echo which passed over the mountain area appeared about 5 mm in rainfall. This value coincided with the surface observation at the landing point (5 mm by this echo).

The dual Doppler radar analysis revealed that the mountain effects were barrier effect for the echo to develop vertically from the surface to the height just above the mountain top and change the wind field to go around the mountain area up to 1 km above the mountain, this result means that the wind field caused the echo propagation to the specific direction under a certain environmental wind field. It is thought therefore that these two effects are important for the concentrated heavy rainfall in limited area especially close to a mountain.

This study will help to understand the heavy rainfall event during the late period of the Baiu season.

Acknowledgments

The authors express their thanks to the member of Meteorological Laboratory, Faculty of Science, Hokkaido University, to help the radar observations. And they also thank to the Typhoon Division of Meteorological Research Institute, JMA for offering Doppler radar data. The expense of this study was supported by the Grant-in-Aid for Scientific Research of the Ministry of Education, Science, and Culture of Japan.

References

Akiyama, T., 1984a. A medium-scale cloud cluster in a Baiu front. Part I: Evolution process and fine structure. J. Meteor. Soc. Japan, **62**, 485-504.

Akiyama, T., 1984b. A medium-scale cloud cluster in a Baiu front. Part II: Thermal and kinematic fields and heat budget. J. Meteor. Soc. Japan, **62**, 505-521.

Asai, T., 1990. A study of mechanism and prediction of heavy rainfalls during rainy season in Japan. Grant-in-Aid for Natural Disaster Science, Ministry of Education, Science, and Culture of Japan, 458 pp.

Brown, E.N. and R.R. Braham Jr., 1963. Precipitation measurements in cumulus congestus. J. Atmos. Sci., **20**, 23-28.

Harimaya. T., S. Kato and K. Kikuchi, 1989. On the confluent phenomena of radar echoes. J. Fac. Sci., Hokkaido Univ., Ser. VII, 8, 323-332.

Kato, S. and T. Harimaya, 1989. Movement and propagation of clusters of cumulonimbus clouds associated with heavy rainfall. J. Fac. Sci., Hokkaido Univ., Ser. VII, 8, 301-322.

Kikuchi, K., O. Ohguchi, H. Uyeda, T. Taniguchi, F. Kobayashi, K. Iwanami, and R. Shirooka, 1994. Rainfall characteristics around Mt. Yotei, Hokkaido. Geophys. Bull. Hokkaido Univ., **57**, 35-59.

Ogura, Y., T. Asai and K. Dohi, 1985. A case study of a heavy precipitation event along the Baiu front in northern Kyushu, 23 July 1982: Nagasaki heavy rainfall. J. Meteor. Soc. Japan, **63**, 883-900.

Takahashi, N., 1994. Studies of the mesoscale and microscale features of heavy rainfall events during the late period of the Baiu season. Doctor thesis of Hokkaido University, 222 pp.

Takahashi, N. and H. Uyeda, 1995. Doppler radar observation on the structure and characteristics of tropical clouds during TOGA-COARE IOP in Manus, Papua New Guinea — Fundamental characteristics of tropical clouds through three case studies on November 23 and December 16, 1992 —. J. Meteor. Soc. Japan, **71** (submitted).

Takeda, T. and H. Iwasaki, 1987. Some characteristics of mesoscale cloud clusters observed in east Asia between March and October 1980. J. Meteor. Soc. Japan, **65**, 507-513.

Tao, W.-K. and J. Simpson, 1989. A further study of cumulus interactions and mergers: Three-dimensional simulations with trajectory analyses. J. Atmos. Sci., **46**, 2974-3004.

Watanabe, H. and Y. Ogura, 1987. Effects of orographically forced upstream lifting on mesoscale heavy precipitation: A case study. J. Atmos. Sci., **44**, 661-675.

Westcott, N.E. and P.C. Kennedy, 1989. Cell development and merger in an Illinois thunderstorm observed by Doppler radar. J. Atmos. Sci., **46**, 117-131.